Time Domain Geoacoustic Inversion using Ship Noise

Cheolsoo Park Woojae Seong
Dept. of Naval Architecture and Ocean Eng., Seoul National University, Seoul 151-742, Korea
Peter Gerstoft David Battle
Marine Physical Lab., Scripps Inst. of Oceanography, Univ. of California, San Diego, La Jolla, CA 92093
Peter Nielsen
SACLANT Undersea Research Centre, 19138 La Spezia, Italy

***Abstract*- A time domain geo-acoustic inversion method using ship noise received on a towed horizontal array is presented. The received signal, containing ship noise, is time-reversed and then back-propagated to the vicinity of the ship. The back-propagated signal is correlated with the received signal which is expected to peak at the ship's location in case of a good match for the environment. This match is utilized for the geoacoustic parameter inversion. The objective function for this optimization problem is thus defined as the normalized power focused in an area around the source position, using a matched impulse response filter. The GA optimization method is applied to the global search problem. The inversion method is first applied to synthetic data and later to experimental data of MAPEX 2000, conducted north of the island of Elba.**

I. INTRODUCTION

Research activities on geo-acoustic inversions have grown due to the significance of the bottom interaction for shallow water sound propagation in the ocean. As a result, various techniques to estimate the geo-acoustic parameters of the ocean bottom via remote sensing have been developed, since direct measurements of the sub-bottom properties are costly and time consuming.

A majority of the inversions in underwater acoustics have been performed using long-range propagation data received on a vertical line array (VLA), and produce spatially averaged output. In order to avoid this degradation of resolution, towed horizontal line array (HLA) inversion schemes have been proposed and implemented [1-4]. Most of the analyses with these data are processed in the frequency domain, both narrowband and broadband, except for some that have chosen to deal directly in the time domain [4-10]. The inversion is usually formulated as an optimization problem enabling various optimization techniques to be applied to the inverse problem, such as global optimization [11, 12] and a hybrid form of global and local search [13, 14].

Most areas of the ocean, especially in shallow waters, show varying seabed characteristics that require range-dependent parameterizations for geo-acoustic inversion. However, a full range-dependent inversion that identifies the ocean bottom structure simultaneously is not tractable thus far due to computational burden in forward modeling. Therefore, simplification of the range dependence into local segments of range independent sectors is a practical method. Experimental implementation via a towed HLA system, which possesses additional advantages of mobility and manageability compared to a VLA, is a possibility [2-4].

Broad-band inversions which utilize the full structure of the bottom reflected signals usually require well controlled acoustic sources. Such dedicated sources may add extra burdens to an inversion experiment. Contrary to controlled sources, tow ship noise which comprise of mechanically generated tonal components and hydrodynamically induced continuous spectra can be a good alternative source for inversion [3, 15].

A time domain inversion using ship noise acquired on a towed HLA is proposed in this paper. An objective function is defined using a matched impulse response filter for the unknown source signal and the filtered output is implemented by back-propagating the time-reversed signal using a ray-based model. Then, a series of global and local searches are applied to both synthetic and measured data in order to find the optimum parameters of the inverse problem.

II. MATCHED IMPULSE RESPONSE FILTER

It has been demonstrated that the sound wave received by a hydrophone and retransmitted backwards focuses at the source position [16]. This phenomenon can be implemented numerically using a received signal as a virtual source, which was utilized in source localization [17, 18]. The wave focusing is explained via matched filtering and array processing.

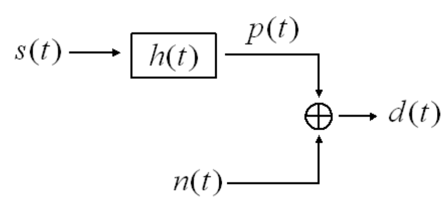

Fig.1. An idealized system of data acquisition.

A data acquisition process can be represented by an idealized system of Fig. 1, where the received signal $d(t)$ comprises of propagated signal $p(t)$ and noise $n(t)$. In linear time invariant system, the propagation of source signal $s(t)$ through a medium can be simply expressed by convolution with an impulse response $h(t)$ as

$$\begin{aligned} d(t) &= p(t) + n(t) \\ &= s(t) * h(t) + n(t) . \end{aligned} \tag{1}$$

The rigorous impulse response for wave propagating in the ocean can be found by solving the wave equation. However, for a set of source and receiver separated within a few water depths, the received signal can be approximated by the sum of eigen-rays weighted and delayed according to their propagation paths. Thus, ignoring the noise for the moment, the received signal is expressed as,

$$\begin{aligned} d(t) &= s(t) * h(t) \\ &= s(t) * \sum_{i=1}^{M} a_i \delta(t - \tau_i) \ , \end{aligned} \tag{2}$$

where a_i and τ_i represent amplitude decay and travel time of the signal component which are propagated through M different paths (eigen-rays), respectively.

If this signal is time reversed and back propagated, then the medium impulse response simply becomes $h(-t)$, called matched impulse response. Applying this filter produces an output at the source location given by

$$\begin{aligned} f(t) &= d(t) * h(-t) \\ &= \sum_{i=1}^{M} a_i^2 s(t) + \sum_{i=1}^{M} \sum_{j \neq i}^{M} a_i a_j s\left(t - (\tau_i - \tau_j)\right) \ . \end{aligned} \tag{3}$$

It can be seen from (3) that the filter output comprises of two components, $\sum_{i=1}^{M} a_i^2 s(t)$ and $\sum_{i=1}^{M} \sum_{j \neq i}^{M} a_i a_j s\left(t - (\tau_i - \tau_j)\right)$, which correspond to a mainlobe and multiple sidelobes of the signal, respectively.

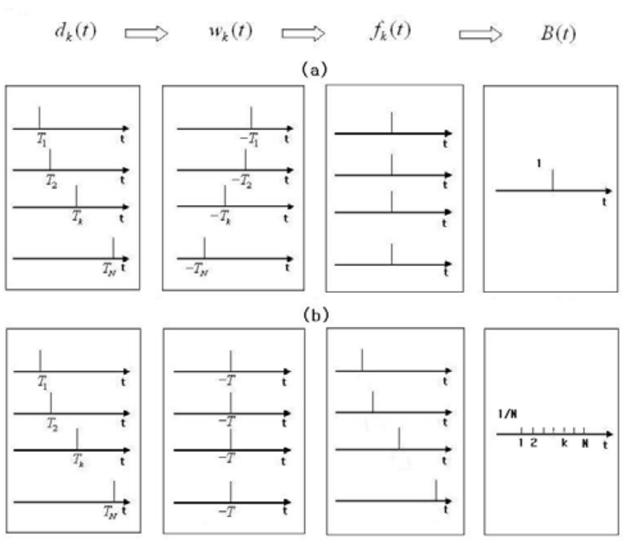

Fig.2. Examples of beamforming using an impulse signal;
(a) optimally beamformed signal and
(b) nonoptimally beamformed signal.

Now, the plane-wave beam-forming concept can be extended for an array with N receivers such that the back-propagated output power is defined as

$$\begin{aligned} B(t) &= \frac{1}{N} \sum_{k=1}^{N} f_k(t) \\ &= \frac{1}{N} \sum_{k=1}^{N} \sum_{i=1}^{M} a_{i,k}^2 s(t) + \frac{1}{N} \sum_{k=1}^{N} \sum_{i=1}^{M} \sum_{j \neq i}^{M} a_{i,k} a_{j,k} s\left(t - (\tau_{i,k} - \tau_{j,k})\right). \end{aligned} \tag{4}$$

When the filter is correct, the mainlobe will be reinforced whereas the sidelobes are cancelled by destructive interference. Therefore, the mainlobe will become dominant over the sidelobes as the number of channels increase (Fig. 2(a)). If the filter is presumed incorrectly, which corresponds to an environmental mismatch, there will be multiple mainlobes along with additional sidelobes (Fig. 2(b)).

The ocean environment itself can be considered as a filter when the received signal is retransmitted reversely. Therefore, when the environment and also the source receiver configurations are modeled as when the signal was recorded at the receiver array, the retransmitted signal will be focused at the original source position.

III. GEOACOUSTIC INVERSION USING SHIP NOISE

Acoustic signals transmitted by a source convey information of the medium through which they propagated. There are numerous acoustic sources for ocean experiments, and the noise generated by a ship is one which will be present most of the time when experiments are carried out in the ocean. If the waveform of a ship noise is unknown, only the impulse response can be used in the geoacoustic inversion.

Inversion parameters which describe the environment are represented by a model vector $\overline{\mathbf{m}} = [\overline{m}_1, \overline{m}_2, \cdots\cdots, \overline{m}_L]^T$, where $[\cdot]^T$ is a transpose operator. The normalized filter output of the channel is defined as

$$f_k(t, \overline{\mathbf{m}}) = \frac{d_k(T - t)}{\sqrt{\int_{-\infty}^{\infty} \left| d_k(T - t) \right|^2 dt}} * \frac{\overline{h}_k(t, \overline{\mathbf{m}})}{\sqrt{\int_{-\infty}^{\infty} \left| \overline{h}_k(t, \overline{\mathbf{m}}) \right|^2 dt}}, \tag{5}$$

where $\overline{h}_k(t, \overline{\mathbf{m}})$ is an impulse response of the corresponding environment. Equation (5) is implemented by propagating the received and time-reversed signal through the environment using a ray-based forward model. The ray-based model [4] is suitable for simulating near field signals. The objective function to be minimized for the inversion using N receivers is defined as

$$\phi = 1 - \max\left(\frac{1}{\Delta T} \int_{T_1}^{T_1 + \Delta T} \left| B(t, \overline{\mathbf{m}}) \right|^2 dt \right), \quad 0 \le T_1 \le T - \Delta T, \tag{6}$$

where

$$B(t,\overline{\mathbf{m}}) = \frac{1}{N}\sum_{i=1}^{N} f_i(t,\overline{\mathbf{m}}). \qquad (7)$$

If the source signal is known *a priori*, the matched impulse response $\overline{h}_k(t,\overline{\mathbf{m}})$ in (5) can be replaced by a matched signal using (6). Examples of the two different filter outputs are shown in Fig. 3. Let's assume an environment whose impulse response in a channel is given by Fig. 3(a). If a source transmits an impulse signal, the impulse response becomes the received signal at the same time and the filtered output for the exact environment is given by Fig. 3(b). Meanwhile, Fig. 3(c) shows the received signal for a source which emits a one-cycle sine function with a frequency of 14 samples, and the outputs of the matched signal filter and the matched impulse response filter using the true parameters are given in Fig. 3(d) and (e), respectively. Comparing the two figures, maximum value occurs at different time and their amplitudes are different to each other, since the source wave form is not considered in the matched impulse response filter. The maximum amplitude in (5) will approach one as the source signal gets closer to an impulse. However, if the model parameters are mismatched to the true environment, the maximum value of the filtered output is reduced as in Fig. 3(f). In addition, the positions of the maximum values for the different channels will be inconsistent, which result in a destructive interference in (7). Therefore, the value of the objective function in (6) will be larger than that of true parameters.

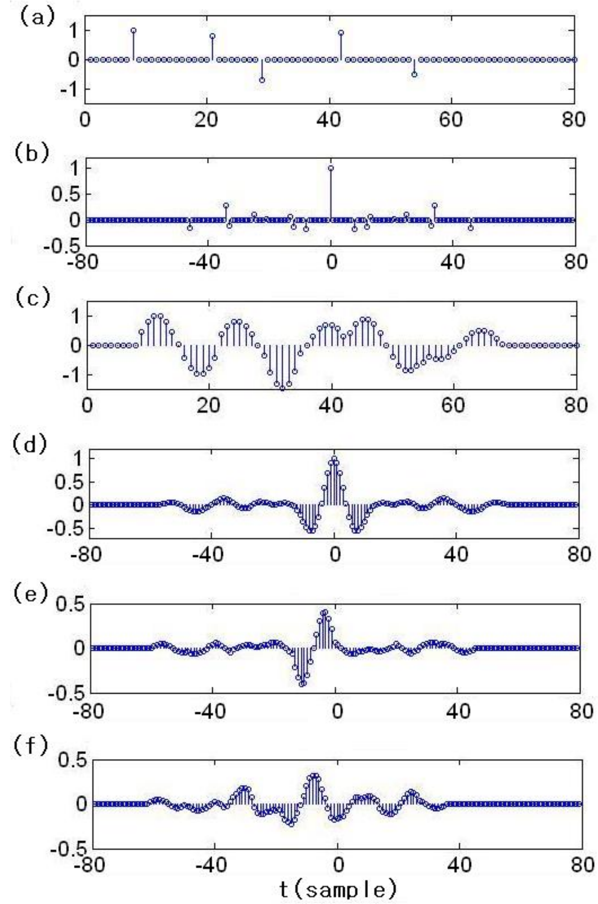

Fig. 3. Examples which illustrate the objective functions; (a) a simulated impulse response, (b) filtered output for an impulse source with true parameters, (c) a simulated measured signal of 1-cycle sine wave, (d) an output signal of the matched signal filter for (c) with true parameters, (e) an output signal of the matched impulse response filter for (c) with true parameters, (f) an output signal of the matched impulse response filter for (c) with mismatched parameters.

IV. EXPERIMENT & ENVIRONMENTAL MODELING

The ship noise experiment was conducted by the SACLANT Undersea Research Center near the island of Elba on November 29 [2]. The data were received by a 254m long HLA for 10 seconds every 30 seconds. The HLA is composed of 128 receivers with 2m separations, and every fourth receiver data (32 receivers) were used for the inversion. During the experiment, the HLA was towed by the R/V *Alliance* and the R/V *Manning* followed approximately 900m behind. Since the distance between the *Alliance* and the nearest receivers to her was approximately 330m, the horizontal range of the Manning from the tail of the array is estimated to be 300m. The bathymetry showed slow growth from 116m to 124m for the entire track and the sound speed of the water column was almost constant at 1520 m/s.

The experimental sites have been studied for a long time and the bottom properties are well known [3]. The bottom comprises of a flat thin layer and a subbottom. The layer thickness is 2.5m and the nominal p-wave speed and density of the subbottom are 1580m/s and 1.8 g/cm^3, respectively. From these considerations, the environmental model of the inversion is set to be range-independent with a single acoustic bottom.

Even though the towed HLA is devised to be neutrally buoyant in the water, it is susceptible to deformations in shape during operations. Therefore, the array shape needs to be included in the inversion parameters for reliable inversion results. Battle *et al*. [3] implemented the array shape deformation by defining the receiver depth as

$$z_i = \alpha\left(1-\left(\frac{2x_i}{L}\right)^2\right) - x_i \sin\theta, \qquad (8)$$

where x_i and z_i are the relative positions of the receiver with respect to the center of the array whose length is L. The inversion parameters α and θ in Eq.(12) represent the array bow and tilt, respectively. The same definition will be adopted for our inversion.

As a consequence, total of eight parameters will be inverted in subsequent inversions; source depth, distance between the source and the nearest receiver, depth of the array center, array tilt, array bow, water depth, bottom sound speed, and bottom density. The attenuation of bottom is excluded in the inversion due to its extremely low sensitivity.

V. INVERSION – THE NUMERICAL SIMULATION

Before applying the inversion scheme to the experimental data, a preliminary inversion using simulated data is performed. The source signal is assumed to be comprised of a 320 Hz tonal component plus a random noise signal. An additional white noise is added to the received signal so as that the ratio of its power to that of the noise free data becomes approximately 15dB.

The inversion results are obtained via an optimization process which searches the parameters to minimize the objective function (6). Direct and surface reflected signals usually have large amplitudes. But they contain only the geometric information, such as the source and receiver positions, and thus are not useful for the inversion of bottom properties. If the geometry and bottom properties are inverted simultaneously, geometrical parameters will dominate over bottom parameters in the search process. In order to prevent such dominance in the optimization, the parameters are inverted separately based on their sensitivities as follows.

At first, the genetic algorithms are applied to the sensitive parameters; the source depth, the array configurations and the water depth, and others fixed at certain values. After one generation of GA is constructed, via selection-crossover-mutation process, the remaining parameters are optimized using a local search method while already optimized parameters are kept at the best values among the population. And the GA search for next generation is performed again with the insensitive parameters fixed at optimal values of the local search. The above two-step search process is repeated until a pre-determined number of generations.

In the inversion for the simulated data, the GA searches are performed for 50 generations and each generation contains 60 populations. The crossover and mutation occur in GA with probabilities of 0.9 and 0.05, respectively. Powell method [19] is used as the local optimizer due to its simplicity.

The inversion results are presented in Fig. 4. The true parameter values of the environment are represented by dashed lines in the figures. Although 1-D marginal *a posteriori* probability display of the results is a common practice [11], we plotted all objective function values with respect to the corresponding parameter values visited during the GA search without any post processing. By doing so, we can obtain information about the optimizer (GA) such as its behavior related to the parameter sensitivity and sampled parameter space. For the insensitive bottom parameters, which are main targets of the inversion, we reevaluated the objective functions based on the best results of GA and showed them in 2-D contour plot of Fig. 4.

It is evident from the results that the matches between true and estimated parameters are consistent with the sensitivity of corresponding parameters. In addition, the overall results seem to be promising considering the low SNR of the data.

VI. INVERSION – THE EXPERIMENTAL DATA

There were two available sources, *Alliance* and *Manning*, in the experiment. Between them, the *Manning* data measured on 08:03:30, 08:07:00, and 08:07:30 UTC are considered in this paper. A data set contains 10 second signals. We divided each signal into 5 segments and applied the inversion scheme to all of them.

Frequent traffic was reported near the experimental site and the data are possibly contaminated by other ships. Therefore, it is recommended to reduce the unwanted interferences using a wavenumber filter [3]. Considering a linear aperture which is aligned along x direction, a signal can be expressed by

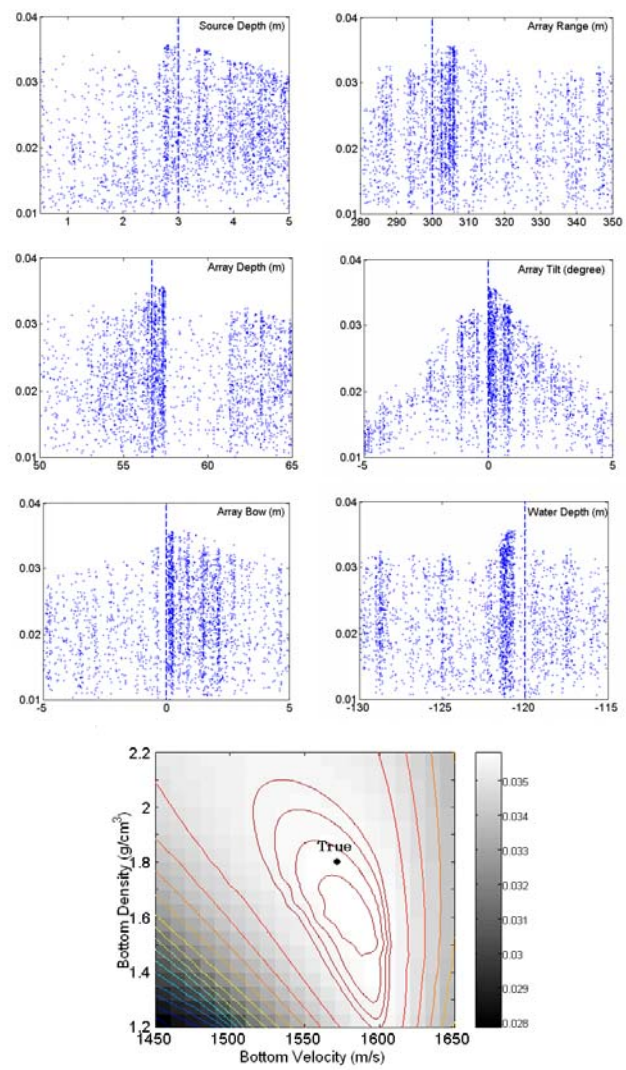

Fig. 4. Inversion results of simulated data.
(Dashed lines represent true values.)

$$p(t,x) = \mathrm{Re}\left(\int_{-\infty}^{\infty}\int_{-\infty}^{\infty} P(\omega,k_x)\exp\left(i(\omega t - k_x x)\right)d\omega dk_x\right), \quad (9)$$

where

$$P(\omega,x) = \frac{1}{4\pi^2}\int_{-\infty}^{\infty}\int_{-\infty}^{\infty} p(t,x)\exp\left(-i(\omega t - k_x x)\right)dtdx, \quad (10)$$

ω is the angular frequency and k_x is the wavenumber with respect to x direction. Since the wave number is related to the incident angle of the wave component by

$$k_x = \frac{\omega}{c}\cos(\theta_i), \quad (11)$$

we can construct a new signal using the propagating components in a particular direction by

$$p_\Omega(t,x) = \mathrm{Re}\left(\int_{-\infty}^{\infty}\int_{k_x\subset\Omega} P(\omega,k_x)\exp\left(i(\omega t - k_x x)\right)d\omega dk_x\right), \quad (12)$$

where Ω means a pertinent wavenumber set.

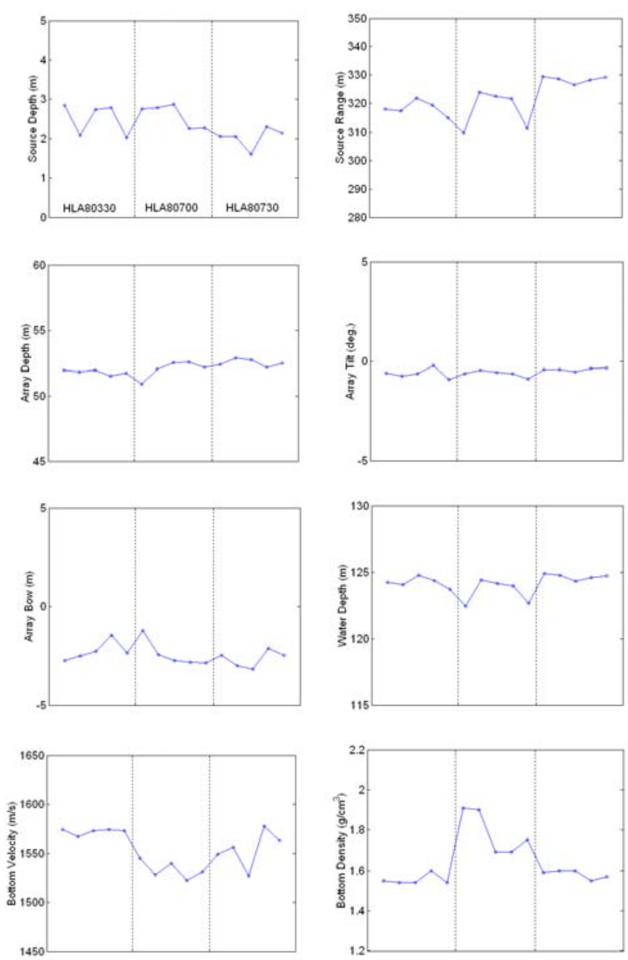

Fig. 5. Inversion results for *Manning* data.

The wavenumber filter in (12) is implemented by a 2-D FFT for discrete time signals in a line array. When the wavenumber filtered data are used in the objective function (6), the simulated impulse response should also include only the corresponding rays.

Fig. 5 shows the inversion results using the *Manning* data which are filtered to contain the rays propagating with incident angles within 50°. The inversion procedure is the same as with the simulated data. The overall results in Fig. 5, especially for sensitive parameters, show a consistent value for the entire data set. However, the inverted bottom properties reveal less consistency than others, which is due to weak sensitivities of the amplitude related parameters as described previously.

Fig. 6 shows the inversion results in 1-D scattered plots for sensitive parameters and in 2-D contour plot for bottom properties using a segment of the data measured at 08:07:30 UTC. Finally, a source localization using other inverted parameters is performed in order to validate the inversion results of Fig. 6. The ambiguity surface in Fig. 7 shows a good focusing of the back propagated signals to the source position.

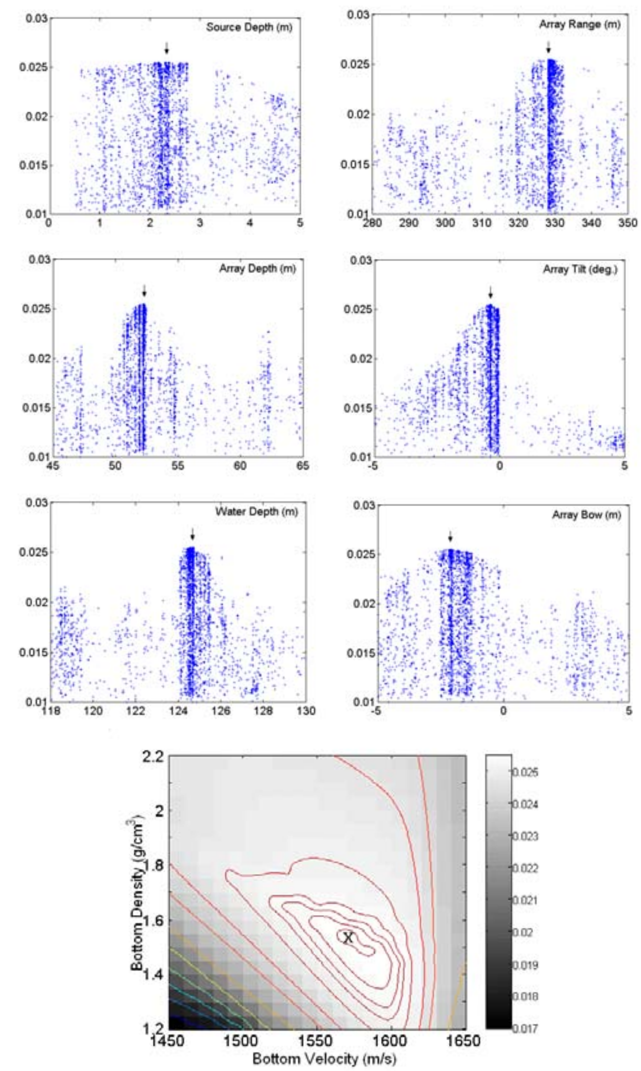

Fig.6. Inversion results for data measured at 08:07:30 UTC. (Arrows and cross represent best solutions.)

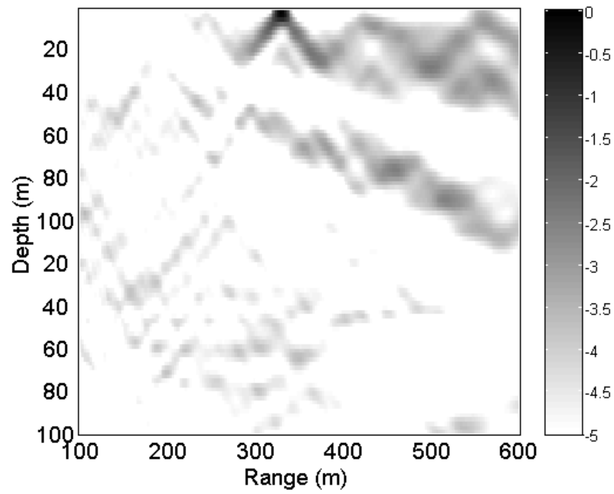

Fig. 7. Ambiguity surface (dB) of the source localization test using data measured at 08:07:30 UTC.

VIII. CONCLUSION

Predicting bottom properties is important for various acoustic applications in shallow waters due to the significance of the bottom interaction. This paper describes a feasible geoacoustic inversion method using a simple towed system consisting of ship noises and a HLA.

The objective function was defined using a matched impulse response filter for the unknown source signal. The filtered output was implemented by back-propagating the received and time-reversed signals using a ray-based forward model. Then, a series of global and local searches was performed using GA and Powell method, respectively, to find the optimum parameters.

The inversion result using synthetic data validated the proposed inversion method. In addition, the present method was applied to the experimental data of MAPEX2000. Fifteen segments of the *Manning* data were inverted and their results showed good consistency, especially for sensitive parameters. From the inversions with experimental data, we have found that the time domain geoacoustic inversion using a simple towed system and ship noise will yield reliable results.

References

[1] W. A. Kuperman, M. F. Werby, K. E. Gilbert, and G. J. Tango, “Beam forming on bottom-interacting tow-ship noise,” IEEE J. Oceanic Eng., 10, 290-298, Jan 1985.

[2] M. Siderius, P. Nielsen, and P. Gerstoft, “Range-dependent seabed characterization by inversion of acoustic data from a towed receiver array,” J. Acoust. Soc. Am., 112, 1523-1535, 2002.

[3] D. Battle, P. Gerstoft, W. A. Kuperman, W. S. Hodgkiss, and M. Siderius "Geoacoustic inversion of tow-ship noise using matched-field processing," IEEE J. Oceanic Eng., 28, July 2003.

[4] C. Park, W. Seong, P. Gerstoft, and M. Siderius, "Time domain geoacoustic inversion of high-frequency chirp signal from a simple towed system," IEEE J. Oceanic Eng., July 2003.

[5] D. P. Knobles and R. A. Koch, “A time series analysis of sound propagation in a strongly mutipath shallow water environment with an adiabatic normal mode approach,” IEEE J. Oceanic Eng., 21, pp. 290-298, 1985.

[6] J-P. Hermand, “Broad-band geoacoustic inversion in shallow water from waveguide impulse response measurements on a single hydrophone: theory and experimental results,” IEEE J. Oceanic Eng., 24, pp. 41-66, 1999.

[7] L. Jaschke and N. R. Chapman, “Matched field inversion of broadband data using the freeze bath method,” J. Acoust. Soc. Am., 106, pp. 1838-1851, 1999.

[8] C. W. Holland and J. Osler, “High-resolution geoacoustic inversion in shallow water: a joint time- and frequency-domain technique,” J. Acoust. Soc. Am., 107, pp. 1263-1279, 2000.

[9] P. Pignot and N. R. Chapman, “Tomographic inversion of geoacoustic properties in a range-dependent shallow-water environment,” J. Acoust. Soc. Am., 110, pp. 1338-1348, 2001.

[10] N. R. Chapman, J. Desert, A. Agarwal, Y. Stephan, X. Demoulin, “Estimation of seabed models by inversion of broadband acoustic data,” Proc. 6th ECUA, Gdansk, pp. 477- 481, 2002.

[11] P. Gerstoft, “Inversion of seismoacoustic data using genetic algorithms and *a posteriori* probability distribution,” J. Acoust. Soc. Am., 95, 770-782, 1994.

[12] S. E. Dosso, M. L. Yeremey, J. M. Ozard, and N. R. Chapman, “Estimation of ocean-bottom properties by matched-field inversion of acoustic field data,” IEEE J. Oceanic Eng., 18, pp. 232-239, 1993.

[13] P. Gerstoft, “Inversion of acoustic data using a combination of genetic algorithm and the Gauss-Newton approach,” J. Acoust. Soc. Am., 97, pp. 2181-2190, 1995.

[14] M. R. Fallat and S. E. Dosso, “Geoacoustic inversion via local, global, and hybrid algorithms,” J. Acoust. Soc. Am., 105, pp. 3219-3230, 1999.

[15] N. R. Chapman, R. M. Dizaji, and R. L. Kirlin, “Geoacoustic inversioln using broad band ship noise,” in Proc. 5th ECUA, Lyon, pp. 787-792, 2000.

[16] A. Parvulescu and C. S. Clay, “Reproducibility of signal transmission in the ocean,” Radio Electron. Eng., 29, pp. 223-228, 1965.

[17] C. S. Clay, “Optimum time domain signal transmission and source location in a waveguide,” J. Acoust. Soc. Am., 81, pp. 660-664, 1987.

[18] R. K. Brienzo and W. S. Hodgkiss, “Broadband matched-field processing,” J. Acoust. Soc. Am. 94(5), pp. 2821-2831, 1993.

[19] M. D. Powell, “A direct search optimization method that models the objective and constraint functions by linear interpolation,” in Advances in Optimization and Numerical Analysis, edited by S. Gomez and J-P. Hennart, Kluwer, Netherlands, 1994, pp. 51-67.